THE MAGNESIUM Mg_2 INDEX AS AN INDICATOR OF METALLICITY IN ELLIPTICAL GALAXIES[1]

ALBERTO BUZZONI AND GIORGIO GARIBOLDI
Osservatorio Astronomico di Brera, Via Brera, 28 20121 Milano, Italy

LUCIANO MANTEGAZZA
Dip. di Fisica Nucleare e Teorica, Università di Pavia, Via Bassi, 6 27100 Pavia, Italy
Received 30 September 1991; revised 29 January 1992

ABSTRACT

A quantitative calibration of the Mg_2 index [Faber *et al.*, AJ, 82, 941 (1977)] is attempted deriving a metallicity scale for elliptical galaxies. The dependence of the index on stellar temperature, gravity, and metallicity has been studied through spectroscopic observations of 87 standards applying the derived calibration to models for stellar population synthesis. Buzzoni's [ApJS, 71, 817 (1989)] computational code has been used to explore the behavior of the index versus age, IMF, and metallicity of simple stellar populations (SSPs) inferring galactic metallicity for the Davies *et al.* [ApJS, 69, 581 (1987)] extensive observational database. It appears that ellipticals are old metal-rich systems, with age about 15 Gyr and [Fe/H] = +0.15. A large spread of nearly one order of magnitude is however derived for metallicity among single galaxies confirming that [Fe/H] is the driving parameter inducing the color spread in the galaxy population. Evolutionary behavior of Mg_2 is briefly discussed giving its expected variations at early epochs for comparison with high-redshift galaxies.

1. INTRODUCTION

Although based on a supposedly confident and simple interpretative scenario, the present understanding of the overall properties of the elliptical galaxies cannot yet firmly overcome the problem of a univoke estimate of the age and chemical composition of their stellar populations. The reason for such uncertainties is that changes in age or metallicity cause similar variations in the photometric properties of their stars.

While for the Galactic globular clusters a direct inspection of the C–M diagram (looking for example at the location of the main sequence turn off point as well as at that of the red giant branch) would allow us to disentangle the problem, for distant galaxies this cannot be done, and we always have to deal with the integrated photometric properties of these stellar aggregates.

Narrowband spectrophotometric indices could be potentially powerful tools since they can be made to work in a selective way within the stellar populations depending on specific ranges for temperature, gravity, and metallicity of the stellar contributors (Spinrad & Taylor 1969; Faber *et al.* 1985; Rose 1985). Therefore, combining a proper number of spectral indices one could imagine, in principle, to be able to disaggregate the different effects and single out the relevant distinctive parameters of the overall evolutionary status of the galaxies.

Among others, the Mg_2 index of Magnesium (Faber *et al.* 1977) is probably the most popular one since it is present in spectra of elliptical galaxies and cool Galactic stars as a very prominent absorption feature about 5200 Å.

Its relationship with the fundamental parameters of stars has been investigated from the theoretical point of view using model atmospheres by Mould (1978), Barbuy (1989), and Gulati *et al.* (1991), while an empirical calibration via K giant stars is given in Faber *et al.* (1985). Observational databases for Galactic and M31 globular clusters can be found in Burstein *et al.* (1984) and Brodie & Huchra (1990), and a very extended set of measurements for local early type galaxies is available from the work of Davies *et al.* (1987).

A first empirical calibration of Mg_2 versus metallicity for elliptical galaxies has been attempted by Burstein (1979) using a slightly different definition of the index, and Terlevich *et al.* (1981). In both cases, however, a main difficulty conspires against firm quantitative conclusions since extension to high metallicities is reached by crude extrapolation from metal-poor Galactic globular clusters. The emerging evidence from those studies however is that elliptical galaxies seem to have a more enhanced metallicity with respect to globular clusters reaching, and possibly exceeding, the solar value.

This work intends to approach the problem in a more complete way providing a quantitative calibration for Mg_2. The task will be accomplished in two steps. We will first investigate empirically the relationship between the index and the fundamental parameters of a wide grid of Galactic standard stars. This will allow us to derive a detailed calibration for dwarfs and giants. Subsequently, this calibration will provide the basis to synthesize the index for a number of theoretical models of stellar populations exploring its change with varying overall distinctive parameters of the populations.

The present paper is organized as follows: in Sec. 2 we present the observational material relative to the standard stars deriving in Sec. 3 the calibration of Mg_2 versus the stellar parameters. These results will be used in Sec. 4 to derive the synthetic index for a grid of models of stellar populations, and a final calibration versus [Fe/H] for galaxies will be obtained and discussed in Sec. 5. In Sec. 6 we pay specific attention to the problem of the dichotomy between age and metallicity estimates for elliptical galaxies. A complementary discussion about the problem of the galactic red-

[1] Based on observations made at the European Southern Observatory (ESO) La Silla, Chile.

 0004-6256/92/061814-14$00.90

dening is performed in Sec. 7, and finally some relevant evolutionary scenarios for Mg_2 in high-redshift galaxies are briefly presented in Sec. 8. Our conclusions are summarized in Sec. 9.

2. OBSERVATIONS AND DATA REDUCTION

Most of the observational database has been collected during a run in 1988 December at the ESO Observatory (La Silla, Chile) with the 1.5 m telescope. The instrument was equipped with a Boller and Chivens Cassegrain spectrograph with an RCA high resolution CCD detector (ESO CCD No. 13). We used a 600 gr/mm grating which supplied a reciprocal dispersion of 59 Å/mm (ESO grating No. 26). The spectral resolution, as estimated from the FWHM of a monochromatic line, resulted in 3 Å.

A total of 79 stars were observed in this run. In addition, a selected list of eight red dwarfs taken from the Gliese catalog was added to the original sample in a second run on 1989 April to extend the database to very cool stars. These new observations were carried out with the same equipment but due to changes in the spectrograph's Schmidt camera the reciprocal dispersion of the spectra was slightly increased to 65 Å/mm.

The stellar database is reported in Table 1(a). In the table stars are labeled with their HD number with the exception of the red dwarfs of the second run identified by their Gliese number. Spectra were reduced using ESO MIDAS package (see MIDAS Users Guide, Image Processing Group, ESO V4.3, 1988). A quite canonical procedure was adopted removing spurious CCD high-frequency features by dividing by quartz lamp flat fields. Wavelength calibration was then accomplished via He-Ar lamp reference spectra taken after each science exposure. Following the original works by Faber *et al.* (1977) and Faber *et al.* (1985) we did not convert spectra into absolute flux units. The instrumental Mg_2 index was converted into the standard system via comparison with reference objects in common with previous authors. This implicitly intends to account both for the CCD low-frequency response and for any other difference in the data acquisition.

The Mg_2 index was derived following Faber *et al.* (1977). Operationally, it is defined as the difference in magnitude between the instrumental flux in a window, $F_2 = (5156.0 - 5197.25)$ Å centered on the Mg feature, and the pseudo-continuum interpolated from two windows, $F_1 = (4897.0 - 4958.25)$ Å, and $F_3 = (5303.0 - 5366.75)$ Å, at the blue and red sides respectively. Thus we have

$$Mg_2 = -2.5 \log \frac{F_2}{F_1 + 0.61(F_3 - F_1)}. \quad (1)$$

As it can be seen from column 6 of Table 1(a) stellar radial velocities are generally lower than 50 km/s, and only one star has a $V_r > 100$ km/s. Direct tests verified that for the most rapid objects in our sample the Doppler shift did not change Mg_2 by more than a few thousands of mag; therefore we decided not to correct for this effect.

Nine stars in common with Faber *et al.* (1985) allowed us to convert the instrumental index into the standard system. A pretty good match was obtained by simply increasing the instrumental flux in F_3 by 6.6%. In order to match also observations in the second run we used supplementary data for three elliptical galaxies in common with Davies *et al.* (1987), as summarized in Table 1(b). Observations refer to the few arcsec nuclear region of the galaxies, and we compared therefore with the corresponding raw values given by Davies *et al.* (1987) after correction for redshift and adopting the procedure described. We found that our values correlated within ± 0.006 mag after recovering a little systematic shift in excess of 0.025 mag. This offset was therefore subtracted from all of our second run indices. Final results for our stellar and galactic calibrators are displayed in Fig. 1, while adopted indices for the whole database are displayed in column 8 of Tables 1(a) and 1(b) together with the observational uncertainties. Globally, the standard system should be reproduced within ± 0.008 mag at 1σ level.

3. CALIBRATION AND DEPENDENCE ON STELLAR PARAMETERS

In order to study the dependence of Mg_2 on the primary stellar parameters, standard stars were selected among those with reasonably confident values of temperature, gravity, and metallicity. Our sample rests basically on the catalog of Cayrel de Strobel *et al.* (1985). Since Mg_2 is recognized to be stronger in cool stars, we included in the sample spectral types later than F6 spanning a wide range in gravity (KM classes from V to I). This includes therefore main sequence stars cooler than 6000 K, and red giants and dwarfs.

For the Gliese stars in our sample we derived temperatures and gravities from the published infrared indices via Eqs. (5) and (6) of Veeder (1975) and via the equations $\log g = 0.102(V-K) + 4.348 = 0.243(R-I) + 4.474$, derived from the various empirical relations given by the same author. The quantities derived in such a way compare fairly well with the direct estimates as it can be tested on some stars for which comparison is available.

The adopted physical parameters Θ ($\equiv 5040/T$), $\log g$, and [Fe/H] for our stellar sample are listed in columns 3–5 of Table 1(a). In our subsequent analysis however we preferred restricting only to KM classes V-III (74 stars in total) to avoid massive supergiants that show a much larger intrinsic scatter, and because we are mainly interested in synthesizing old stellar populations.

In Fig. 2 the working stellar sample is displayed in the plane ($\log g$, Θ) and compared to a reference isochrone (VandenBerg 1985) and some stellar evolutionary tracks (Becker 1981). As it can be seen we are dealing with a typical disk population having a large spread in mass and age. Distribution in metallicity is displayed in Fig. 3. As expected, most of the stars lie about the solar value with a spread of ± 1 dex and there are only a few metal-poor member. Consequently, our calibration will be especially suitable for metal-rich stellar populations.

In order to extend the database available for stellar calibration we included in our analysis also most of the sample of giant stars observed by Faber *et al.* (1985) for which we were able to recover the physical parameters homogeneously. In total 31 stars were accounted for. This set of data is presented in Table 2 excluding the nine stars in common that already appear in Table 1(a).

It would be useful for our aims to derive an analytical formula describing the dependence of Mg_2 on Θ, $\log g$, and [Fe/H]. This can be done with the help of Fig. 4, where the stellar subsample in the range [Fe/H] $= \pm 0.25$ is compared with equi-levels in Mg_2. For solar metallicity, a confident fit to the data for $Mg_2 \leqslant 0.46$ can be given by

$$Mg_2 = 1.26\Theta + 0.103 \log g - 1.393. \quad (2)$$

TABLE 1(a). Observational sample.

Name	Sp.Type	Θ	log g	[Fe/H]	V_{rad}	$v \sin i$	Mg_2	σ
1581	F9 V	0.84	4.50	−0.10	9	0	0.095	±0.003
1835	G2 V	0.87	4.45	0.05	−7	6	0.129	±0.004
3443	G8 V	0.93	4.57	−0.16	17	2	0.170	±0.003
10380	K3 III	1.26	1.50	−0.33	0	<19	0.317	±0.005
10700	G8 V	0.95	4.46	−0.42	−16	2	0.202	±0.004
13611	G6 II–III	0.98	3.00	0.00	−4	<17	0.105	±0.005
13974	G0 V	0.90	4.50	−0.30	−6	<10	0.149	±0.005
14802	G1 V	0.85	4.40	0.00	18	4	0.096	±0.004
17925	K2 V	0.99	4.50	−0.15	19	–	0.286	±0.004
18322	K1 III	1.07	2.80	0.20	−20	<17	0.219	±0.003
20630	G5 V	0.89	4.45	0.08	20	<17	0.148	±0.004
20766	G3–5 V	0.89	4.10	−0.06	12	–	0.141	±0.005
20794	G8 III	0.93	4.30	−0.29	87	–	0.203	±0.004
20807	G2 V	0.88	4.40	−0.19	12	–	0.111	±0.004
20894	G6.5 IIb	0.99	3.10	−0.20	8	–	0.114	±0.005
22049	K2 V	1.00	4.40	−0.24	16	<17	0.304	±0.003
22484	F9 V	0.84	3.98	−0.09	28	0	0.083	±0.003
30495	G1 V	0.84	4.50	0.10	23	–	0.129	±0.004
30562	F8 V	0.86	3.75	0.13	79	–	0.114	±0.004
32147	K3 V	1.06	4.50	0.02	27	–	0.511	±0.005
33793	M1 V	1.43	4.87	−0.50	0	–	0.558	±0.006
36395	M1 V	1.39	4.80	0.60	0	–	0.457	±0.004
37160	K0 IIIb	1.02	2.57	−0.04	99	–	0.186	±0.004
37763	K2 III	1.05	2.80	0.35	57	–	0.356	±0.004
39091	G1 V	0.89	3.94	0.00	9	–	0.102	±0.004
39364	G8 III	1.08	1.90	0.15	99	0	0.181	±0.003
39523	K1 III	1.08	1.90	0.15	16	–	0.223	±0.004
44033	K3 Ib	1.53	1.00	−0.07	36	–	0.471	±0.005
45829	K0 Iab	1.12	0.20	−0.01	0	–	0.213	±0.005
46407	K0 III	1.01	2.55	0.03	−11	–	0.174	±0.004
47205	K1 III	1.02	3.08	0.07	3	<17	0.284	±0.004
50778	K4 III	1.30	1.90	−0.12	97	<19	0.387	±0.004
50877	K2 Iab	1.20	0.40	0.05	36	<19	0.322	±0.005
56577	K3 Ib	1.15	1.28	0.16	28	–	0.381	±0.004
60219	F6 I–II	1.05	1.70	−0.70	0	–	0.047	±0.003
62576	K3 Ib	1.17	1.30	0.01	33	–	0.420	±0.004
62644	G6 IV	0.98	3.12	−0.35	28	–	0.147	±0.004
63302	K1 Ia–Iab	1.12	0.20	0.17	31	–	0.254	±0.005
65699	cK2	1.04	1.50	−0.20	11	–	0.140	±0.005
69267	K4 III	1.17	1.87	−0.21	22	<17	0.334	±0.004
76151	G3 V	0.90	4.40	−0.02	28	<6	0.138	±0.005
83548	G8 II	1.02	2.00	−0.33	2	–	0.147	±0.006
84810	G5 Iab–Ib	0.99	1.50	0.30	3	–	0.120	±0.005
84903	K0	1.12	0.80	−2.60	0	–	0.048	±0.004
88218	F8 V	0.91	3.36	−0.42	41	–	0.096	±0.005
88284	K0 III	1.00	2.86	0.10	19	<19	0.191	±0.004
89388	K3 IIa	1.12	1.60	0.54	8	–	0.305	±0.004
91324	F6 V	0.83	3.90	−0.60	20	–	0.068	±0.005
91805	G8 II–III	1.04	2.00	−0.10	8	–	0.122	±0.006
95272	K0 III	1.25	2.48	−0.12	47	<19	0.200	±0.004
95345	K1 III	1.08	2.00	−0.05	6	<19	0.209	±0.005
96918	G4 0–Ia	0.88	0.40	0.32	7	23	0.121	±0.004
97907	K3 III	1.32	2.07	−0.17	18	19	0.265	±0.005
98430	G8 III–IV	1.04	2.48	−0.33	−5	<19	0.172	±0.003

TABLE 1(a). (continued)

Name	Sp.Type	Θ	log g	[Fe/H]	V_{rad}	$v \sin i$	Mg_2	σ
99491	K0 IV	0.90	4.60	0.09	−3	–	0.244	±0.005
100407	G7 III	1.04	2.20	−0.10	−5	–	0.152	±0.003
102365	G5 V	0.93	4.09	−0.59	15	–	0.146	±0.005
102634	F7 V	0.83	4.30	0.12	4	6	0.078	±0.005
102870	F9 V	0.83	4.30	0.21	5	3	0.083	±0.004
111631	M0.5 V	1.29	4.50	0.10	0	–	0.506	±0.006
188510	G5 V	0.95	3.80	−1.80	0	–	0.055	±0.007
189567	G3 V	0.88	4.08	−0.28	−12	–	0.112	±0.004
190248	G6–8 IV	0.90	4.31	0.43	−22	–	0.187	±0.003
191408	K3 V	1.03	4.60	−0.07	130	–	0.352	±0.004
192310	K0 V	1.02	4.50	−0.08	−54	–	0.321	±0.004
192947	G8 III	1.01	3.00	0.12	0	<17	0.148	±0.004
196378	F8 V	0.83	4.10	−0.30	−32	0	0.057	±0.004
203638	K0 III	1.11	1.50	0.35	22	–	0.266	±0.004
208776	G0 V	0.85	4.00	−0.26	24	–	0.073	±0.005
209100	K4–5 V	1.12	4.70	0.04	−40	–	0.471	±0.004
211391	G8 III–IV	1.02	2.80	−0.07	−15	<17	0.160	±0.003
212330	G3 IV	0.87	4.20	0.00	8	–	0.118	±0.004
213009	K0 III	1.05	2.00	−0.20	5	–	0.136	±0.005
215104	K0 III	1.06	2.30	−0.20	29	–	0.154	±0.004
216437	G2–3 IV	0.85	4.40	0.10	−3	–	0.130	±0.004
216763	G8 III	1.03	2.50	−0.20	−12	–	0.143	±0.003
219615	K0 III	1.03	2.42	−0.20	−14	7	0.127	±0.004
221148	K3 III	1.07	2.60	0.07	−25	–	0.360	±0.004
225212	K3 Ib	1.21	0.95	0.02	−42	<17	0.329	±0.004
GL 229	M1 V	1.38	4.75	0.2	–	–	0.455	±0.004
GL 234	M7	1.68	4.91	–	–	–	0.519	±0.006
GL 273	M4.5	1.55	4.85	–	–	–	0.508	±0.003
GL 488	M0.5e	1.30	4.70	–	–	–	0.508	±0.003
GL 551	M5e	1.92	5.03	–	–	–	0.618	±0.004
GL 673	K7 V	1.26	4.50	0.4	–	–	0.520	±0.003
GL 699	M5	1.59	4.87	–	–	–	0.599	±0.005
GL 729	M4.5e	1.62	4.89	−0.7:	–	–	0.527	±0.004

TABLE 1(b). Elliptical galaxies.

Name	Type	V_{rad}	Mg_2	σ
NGC 3377	E6	689	0.284	±0.009
NGC 4472	E2	997	0.337	±0.016
NGC 4649	E2	1095	0.358	±0.013

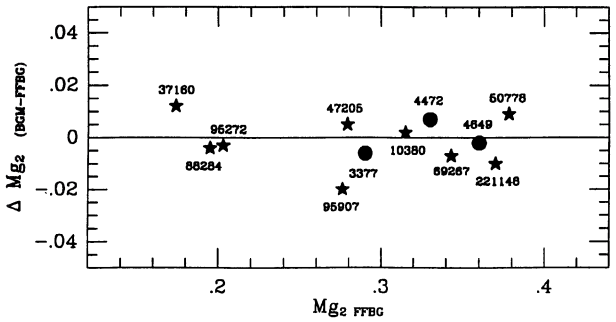

FIG. 1. Comparison between instrumental and standard Mg_2 system for nine stars and three galaxies in common with Faber *et al.* (1985) and Davies *et al.* (1978). Match of the standards is made after corrections for systematic shifts as described in the text. Scatter of the points is $\sigma = \pm 0.008$ mag. ⋆'s indicate stars, labeled with their HD number; ●'s indicate galaxies with their NGC number.

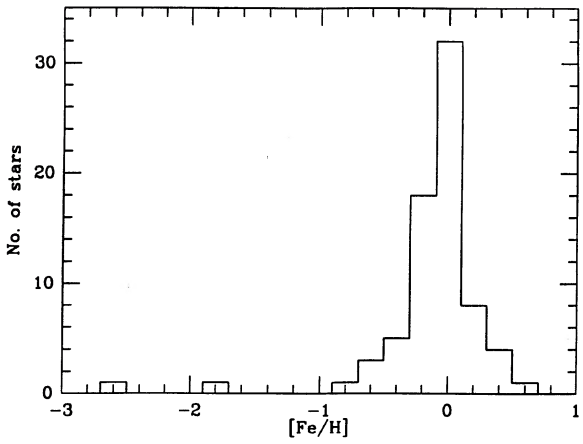

FIG. 3. Metallicity distribution for the 74 stars in our adopted working sample.

As noted also by Mould (1978) and Barbuy (1989), when attempting a theoretical synthesis of the index via model atmospheres at higher values of Mg_2 a saturation occurs in the index due to the increasing importance in the spectra of the TiO blend affecting the pseudo-continuum in the window F_1 (cf. for example the red dwarf spectrum in Fig. 5). This effect works in decreasing artificially the depth of the Mg feature causing a break in the trend of the index. Providing continuity in the analytical fit at $Mg_2 = 0.46$, the saturation regime can be described by

$$Mg_2 = 0.22\Theta + 0.018 \log g + 0.136. \quad (3)$$

The break is well evident in Fig. 6 for main sequence stars (including dwarfs). Furthermore, the trend of Mg_2 versus metallicity can be investigated. We find a mild positive derivative, $\partial Mg_2/\partial [Fe/H] = 0.05$, to be accounted for in the complete set of fitting relations:

$$Mg_2 = 1.26\Theta + 0.103 \log g + 0.05[Fe/H] - 1.393, \quad (Mg_2 \leqslant Mg^*); \quad (4)$$

$$Mg_2 = 0.22\Theta + 0.018 \log g + 0.05[Fe/H] + 0.136, \quad (Mg_2 > Mg^*). \quad (5)$$

The obvious constraint to the equations is that $Mg_2 > 0$, with

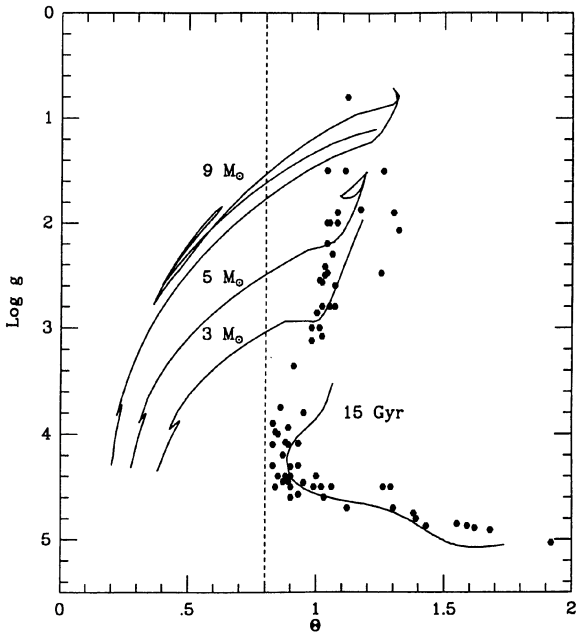

FIG. 2. The stellar working sample (74 stars). Solid lines refer to stellar evolutionary tracks for 3, 5, and 9 $\mathcal{M}_\odot$ after Becker (1981), and with a 15 Gyr isochrone (VandenBerg 1985). A solar metallicity is assumed in the reference models. Vertical dashed line indicates the upper limit for temperature of selected stars in our working sample.

TABLE 2. Extended stellar sample.*

Name	Sp.Type	Θ	log *g*	[*Fe/H*]	*Mg2*
3546	F3 III	1.19	2.44	−0.75	0.119
12929	K2 III	1.12	2.40	−0.20	0.229
19476	K0 III	1.02	3.30	0.08	0.188
34334	K3 III	1.21	2.20	−0.32	0.340
35620	K3 III	1.19	1.60	−0.14	0.361
38751	G8 III	1.27	2.36	−0.11	0.216
58207	G9 III	1.14	–	0.16	0.180
72324	G9 III	1.17	–	0.32	0.149
85503	K2 III	1.12	2.38	0.05	0.327
97907	K3 III	1.32	2.07	−0.17	0.276
113226	G8 III	1.02	2.70	0.02	0.140
122563	F8 IV	1.10	1.20	−2.70	0.028
124897	K1 III	1.18	1.59	−0.50	0.273
129312	G8 III	1.05	2.10	−0.14	0.138
132345	K3 III	1.15	2.30	0.00	0.317
135722	G8 III	1.12	2.50	−0.49	0.147
165195	K4 III	1.16	0.90	−2.30	0.060
180928	K3 III	1.25	1.50	−0.60	0.353
184406	K3 III	1.19	2.44	0.27	0.346
188056	K3 III	1.12	1.85	−0.12	0.382
188512	G8 IV	0.98	3.60	−0.21	0.179
198149	K0 IV	1.05	3.18	−0.17	0.198

* from Faber *et al.* (1985)

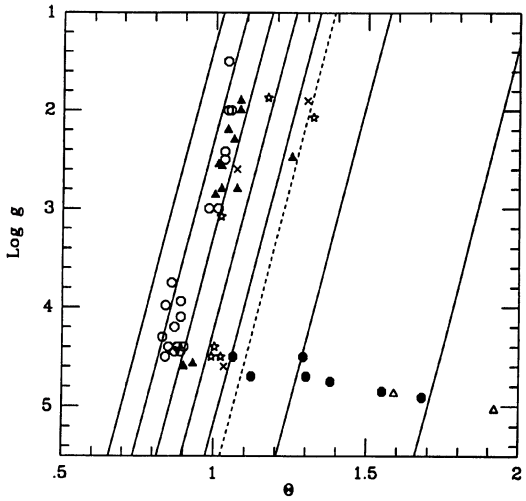

FIG. 4. Comparison between the stellar subsample about solar metallicity ([Fe/H] $\pm$ 0.25 dex, 53 stars) and the fitted Mg_2 equi-levels from Eqs. (2) and (3). Data are sampled in bins of width $\pm$ 0.05 mag centered about $Mg_2 = 0.1$ (○), 0.2 (▲), 0.3 (⋆), 0.4 (×), 0.5 (●), and 0.6 (△). Accordingly, solid lines increase from the left to the right with the same steps. The break in the increasing rate of the index due to saturation about $Mg_2 = 0.46$ is displayed by the dashed line.

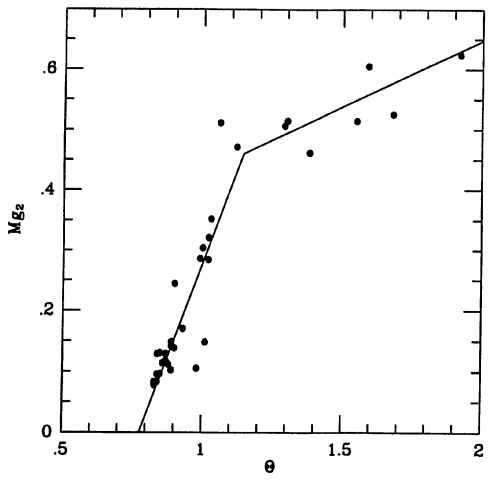

FIG. 6. The effect of the break in the increasing rate of Mg_2 at low temperatures. Displayed are 33 stars from the working sample with metallicity about solar ([Fe/H] = $\pm$ 0.25 dex) and log $g \geqslant 3$. The fitting relation for log $g = 4.0$ is also reported.

a boundary condition at the saturation level, $Mg^* = 0.46 + 0.05[Fe/H]$.

The accuracy of our final Mg_2 calibration can be tested directly in Figs. 7 and 8. Here, (O − C)'s from Eqs. (4) and (5) are plotted versus observed Mg_2 and versus metallicity. For comparison, in the figures we have marked with different symbols our data and those by Faber *et al.* (1985). No systematic trends are evident, and the observed Mg_2 is reproduced within $\sigma(Mg_2) = \pm 0.067$ mag, with our sample slightly less scattered ($\sigma_{BGM} = \pm 0.056$) than that of Faber *et al.* (1985) ($\sigma_{FFBG} = \pm 0.097$).

Since most of the stars fall in the range of Eq. (4), we can infer back from it the upper limits for the formal uncertainties in Θ and log g. By differentiating the relation we derive a 3%–5% scatter for temperature [i.e. $\sigma(\Theta) \leqslant 0.05$] while $\sigma(\log g) \leqslant 0.65$. Our estimates seem to be fully compatible with the typical observational uncertainties for these parameters in the standard stars, and we conclude therefore that most of the apparent scatter on Mg_2 is in fact mainly induced by such external errors supporting therefore the adequacy of our fit.

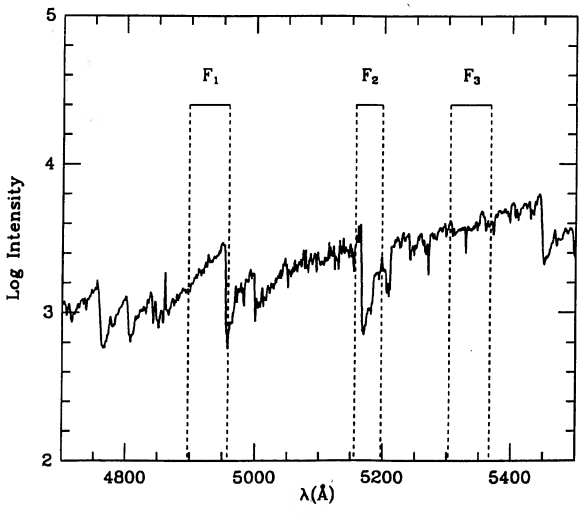

FIG. 5. Selected spectrum for the red dwarf Gliese 551. The three windows involved in the computation of Mg_2 are displayed. It is clearly evident the disturbing effect on F_1 flux due to the molecular blend of TiO.

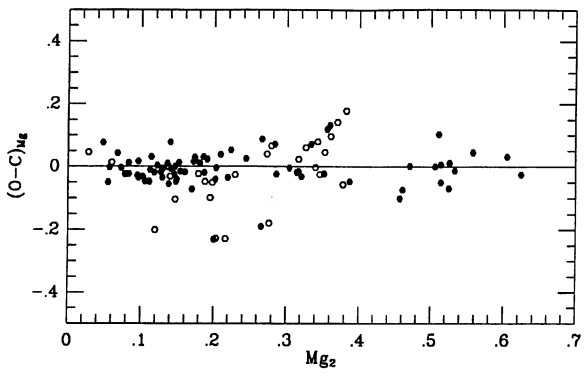

FIG. 7. Residuals from fitting Eqs. (4) and (5) vs observed Mg_2. Full dots represent our working stellar sample (74 stars), while open dots mark Faber *et al.* (1985) extended sample (22 stars). The global standard deviation is $\sigma(Mg_2) = \pm 0.067$ mag, with $\sigma_{BGM} = \pm 0.056$ mag and $\sigma_{FFBG} = \pm 0.097$ mag. No systematic trends are evident respect to Mg_2.

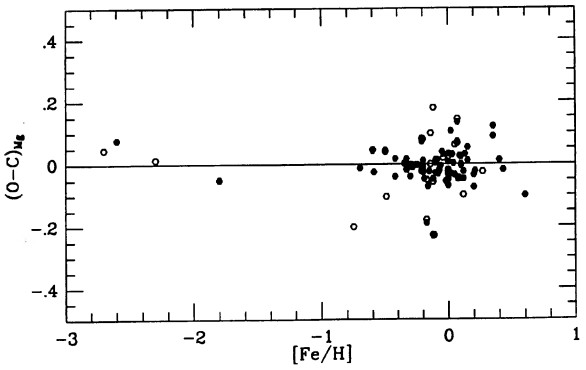

FIG. 8. Same as Fig. 7, but vs [Fe/H]. Once more no systematic trends seem to appear.

4. TOWARD POPULATION SYNTHESIS

After having explored in detail the relationship of Mg_2 with the relevant stellar parameters, we have got now the tool to approach the second step of our task attempting the synthesis of the index for composite stellar aggregates.

It will be especially useful to address our attention to the case of the so-called simple stellar populations (SSPs) in the meaning stated, for example, in Buzzoni (1989). We will refer to them as single generations of coeval stars with fixed metallicity and mass distribution following a power-law IMF. It is clear of course that this straightforward approach could enable us to reproduce any other more complex scenario involving a change in the star formation rate or in the other distinctive parameters of the populations.

In a general way, if we know the value of Mg_2 for a number of single stars, the synthetic index for the whole aggregate will be

$$Mg_2^{(tot)} = -2.5 \log \frac{F_f^{(tot)}}{F_c^{(tot)}}, \tag{6}$$

with

$$\frac{F_f^{(tot)}}{F_c^{(tot)}} = \frac{\sum \left[F_c^{(j)} \times \left(\frac{F_f}{F_c} \right)^{(j)} \right]}{\sum F_c^{(j)}}$$

$$= \frac{\sum \left[F_c^{(j)} \times 10^{-0.4 Mg_2(j)} \right]}{\sum F_c^{(j)}}. \tag{7}$$

Here, j is the index running over the whole population and labels "f" and "c" refer to "feature" and "continuum."

It could be demonstrated that the exact choice of the wavelength for the continuum F_c [last term of Eq. (7)] is not critical, providing to remain close enough to the feature. This only introduces second-order uncertainties on the final synthetic value of the index. The net advantage of this is that we can accomplish synthesis using low-resolution spectral energy distributions (SED) for stars, avoiding to reproduce explicitly any fine detail within the relevant spectral range.

Calculations have been performed for 186 models of SSP using Buzzoni's code for evolutionary population synthesis [the reader is referred to Buzzoni (1988, 1989) for any further computational detail]. Summary of the results is given in Tables 3(a)–3(c). Tables are presented for different values of the IMF power index (s) ranging from 1.35 to 3.35 (in our notation the canonical Salpeter value is 2.35). Each panel is arranged increasing metallicity as first running parameter, and age as second one. For each SSP we give then Mg_2 together with $B-V$ and $V-K$. This is done for two values of the Reimers (1975) parameter η driving stellar mass loss during the evolution along the red and asymptotic giant branches (RGB and AGB). A red clump of stars is assumed throughout in the models for the morphology of the horizontal branch (HB). Direct tests confirmed that bluer HB morphologies would slightly decrease systematically Mg_2 by only a few thousands of mag as Mg_2 is weakly sensitive to stars in this evolutionary phase. Broadband color variations can be evaluated from the complete set of models in Buzzoni (1989).

Again it is useful to have a more compact analytical representation of the data displaying direct relationships between the different parameters. Considering only the relevant range for metal-rich globular clusters and galaxies (i.e. $[Fe/H] \geqslant -1$) a good fit to the models gives

$$Mg_2^{(synt)} = 0.135[Fe/H] + 0.163 \times 10^{\Delta s/28} \log t_9 + (\Delta s^2/220) - 0.015(\eta - 0.3) + 0.09 \tag{8}$$

where t_9 is the age of the SSP in Gyr and $\Delta s = (s - 2.35)$. The equation can reproduce the tabular values of Mg_2 within ± 0.002 mag in the average or ± 0.004 in the worst cases.

TABLE 3(a). SSP models for $s = 1.35$.

			$\eta = 0.3$			$\eta = 0.5$		
Log Z	[Fe/H]	Age (Gyr)	Mg_2	$B-V$	$V-K$	Mg_2	$B-V$	$V-K$
-4.00	-2.27	8.00	0.009	0.47	1.78	0.010	0.46	1.72
		10.00	0.014	0.58	2.03	0.014	0.57	1.98
		12.50	0.019	0.65	2.20	0.019	0.63	2.14
		15.00	0.021	0.67	2.24	0.022	0.65	2.19
		18.00	0.025	0.69	2.28	0.026	0.67	2.22
-3.00	-1.27	8.00	0.075	0.71	2.46	0.072	0.70	2.39
		10.00	0.084	0.73	2.50	0.081	0.72	2.42
		12.50	0.092	0.75	2.51	0.089	0.74	2.43
		15.00	0.099	0.77	2.52	0.095	0.75	2.44
		18.00	0.107	0.78	2.54	0.101	0.76	2.45
-2.00	-0.25	4.00	0.153	0.78	2.91	0.150	0.77	2.81
		5.00	0.168	0.80	2.93	0.165	0.79	2.84
		6.00	0.180	0.82	2.95	0.177	0.81	2.85
		8.00	0.200	0.84	2.97	0.196	0.83	2.87
		10.00	0.214	0.86	3.00	0.211	0.85	2.89
		12.50	0.229	0.88	3.02	0.225	0.87	2.92
		15.00	0.238	0.89	3.04	0.233	0.88	2.92
-1.77	-0.02	4.00	0.184	0.81	3.05	0.181	0.80	2.95
		5.00	0.198	0.83	3.07	0.195	0.82	2.96
		6.00	0.209	0.84	3.08	0.207	0.83	2.97
		8.00	0.229	0.87	3.10	0.227	0.86	3.00
		10.00	0.246	0.89	3.13	0.243	0.88	3.03
		12.50	0.261	0.91	3.17	0.258	0.90	3.05
		15.00	0.271	0.92	3.19	0.267	0.91	3.07
-1.54	0.22	4.00	0.216	0.84	3.18	0.214	0.83	3.08
		5.00	0.227	0.85	3.20	0.225	0.85	3.08
		6.00	0.240	0.87	3.21	0.238	0.86	3.11
		8.00	0.260	0.89	3.24	0.258	0.89	3.14
		10.00	0.277	0.92	3.27	0.274	0.91	3.16
		12.50	0.291	0.94	3.29	0.288	0.93	3.19
		15.00	0.302	0.95	3.33	0.298	0.95	3.21

TABLE 3(b). SSP models for $s = 2.35$.

			$\eta = 0.3$			$\eta = 0.5$		
Log Z	[Fe/H]	Age (Gyr)	Mg_2	$B-V$	$V-K$	Mg_2	$B-V$	$V-K$
-4.00	-2.27	8.00	0.019	0.48	1.84	0.020	0.48	1.76
		10.00	0.026	0.60	2.08	0.027	0.58	2.04
		12.50	0.034	0.66	2.25	0.035	0.64	2.20
		15.00	0.037	0.68	2.29	0.038	0.67	2.24
		18.00	0.042	0.70	2.33	0.043	0.68	2.28
-3.00	-1.27	8.00	0.084	0.71	2.48	0.082	0.70	2.42
		10.00	0.093	0.73	2.52	0.091	0.72	2.45
		12.50	0.103	0.75	2.54	0.100	0.74	2.47
		15.00	0.110	0.77	2.56	0.106	0.75	2.49
		18.00	0.118	0.79	2.59	0.114	0.77	2.51
-2.00	-0.25	4.00	0.155	0.77	2.88	0.152	0.76	2.78
		5.00	0.171	0.79	2.90	0.168	0.79	2.82
		6.00	0.184	0.81	2.93	0.181	0.80	2.83
		8.00	0.205	0.84	2.96	0.202	0.83	2.87
		10.00	0.221	0.86	3.00	0.217	0.85	2.91
		12.50	0.236	0.88	3.03	0.233	0.87	2.95
		15.00	0.246	0.89	3.07	0.242	0.88	2.96
-1.77	-0.02	4.00	0.186	0.80	3.01	0.184	0.79	2.92
		5.00	0.202	0.82	3.05	0.199	0.81	2.94
		6.00	0.214	0.84	3.06	0.211	0.83	2.96
		8.00	0.235	0.86	3.09	0.233	0.86	3.00
		10.00	0.253	0.89	3.14	0.250	0.88	3.04
		12.50	0.269	0.91	3.18	0.266	0.90	3.08
		15.00	0.280	0.93	3.22	0.276	0.92	3.12
-1.54	0.22	4.00	0.218	0.83	3.13	0.216	0.82	3.03
		5.00	0.230	0.85	3.16	0.229	0.84	3.05
		6.00	0.244	0.86	3.18	0.242	0.86	3.08
		8.00	0.266	0.89	3.23	0.264	0.89	3.13
		10.00	0.284	0.92	3.27	0.282	0.91	3.17
		12.50	0.299	0.94	3.31	0.297	0.94	3.21
		15.00	0.311	0.96	3.35	0.308	0.96	3.25

TABLE 3(c). SSP models for $s = 3.35$.

			$\eta = 0.3$			$\eta = 0.5$		
Log Z	[Fe/H]	Age (Gyr)	Mg_2	$B-V$	$V-K$	Mg_2	$B-V$	$V-K$
-4.00	-2.27	8.00	0.044	0.52	2.06	0.046	0.52	2.03
		10.00	0.058	0.63	2.29	0.060	0.62	2.27
		12.50	0.069	0.69	2.43	0.071	0.68	2.39
		18.00	0.078	0.74	2.49	0.080	0.72	2.46
-3.00	-1.27	8.00	0.109	0.74	2.64	0.107	0.73	2.60
		10.00	0.116	0.76	2.66	0.114	0.74	2.61
		12.50	0.127	0.78	2.69	0.125	0.77	2.64
		15.00	0.135	0.80	2.73	0.132	0.78	2.68
		18.00	0.145	0.82	2.76	0.141	0.80	2.70
-2.00	-0.25	4.00	0.165	0.77	2.94	0.163	0.76	2.86
		5.00	0.182	0.80	2.97	0.180	0.79	2.91
		6.00	0.197	0.82	3.01	0.194	0.81	2.94
		8.00	0.219	0.85	3.07	0.217	0.84	3.01
		10.00	0.237	0.88	3.14	0.234	0.87	3.07
		12.50	0.254	0.90	3.20	0.251	0.90	3.13
		15.00	0.265	0.92	3.23	0.261	0.91	3.16
-1.77	-0.02	4.00	0.199	0.81	3.09	0.197	0.81	3.02
		5.00	0.216	0.84	3.14	0.214	0.83	3.06
		6.00	0.228	0.85	3.15	0.226	0.84	3.07
		8.00	0.252	0.88	3.22	0.250	0.88	3.15
		10.00	0.271	0.92	3.28	0.269	0.91	3.21
		12.50	0.289	0.94	3.35	0.286	0.94	3.28
		15.00	0.302	0.97	3.42	0.299	0.96	3.35
-1.54	0.22	4.00	0.229	0.84	3.18	0.228	0.83	3.10
		5.00	0.244	0.86	3.23	0.242	0.85	3.15
		6.00	0.258	0.88	3.27	0.256	0.87	3.19
		8.00	0.281	0.91	3.34	0.280	0.91	3.26
		10.00	0.301	0.94	3.41	0.299	0.94	3.33
		12.50	0.319	0.97	3.49	0.317	0.97	3.42
		15.00	0.332	1.00	3.54	0.330	0.99	3.47

A first important remark stems from a comparison of the Mg_2 calibration for stars [Eqs. (4) and (5)] and for stellar populations [Eq. (8)]. The dependence on metallicity strongly increases for stellar aggregates making the index a very effective tracer for [Fe/H] in SSPs. Actually, two additive contributions magnify such a relationship. The first one is the *direct* dependence of Mg_2 as it appears in Eqs. (4) and (5). The second one is an *indirect* influence due to the fact that increasing metallicity will move redward colors of the population isochrones. This means a lower temperature for stars inducing a dependence on the integrated index via a coherent change of Θ. Since Mg_2 increases for decreasing temperature the two effects work in the same direction. It is worth stressing that such an indirect influence is by far the more relevant one, and actually it happens that Mg_2 becomes a metallicity indicator in SSPs essentially via temperature effects.

5. CALIBRATING GALAXIES

Before proceeding to a quantitative study of the metallicity distribution in elliptical galaxies, we must first try another preliminary but important check involving globular clusters. It is known, in fact, that these stellar systems closely match the concept of SSP allowing a confident comparison with our theoretical calibration. In addition, stellar populations in Galactic globular clusters can be resolved observationally, and a direct measurement of their metallicity can be done directly from spectra of the single stars.

Brodie & Huchra (1990) calibrated Mg_2 index for some of the clusters in the Galaxy and in M31. They compiled data for Galactic primary calibrators from Burstein *et al.* (1984) adopting the metallicity scale of Zinn & West (1984), and extending the calibration to M31 clusters via the IR colors by Aaronson *et al.* (1978) and Frogel *et al.* (1980). For the sake of homogeneity, and also to improve the consistency with the canonical definition of the Mg_2 index we preferred to use the original data from Burstein *et al.* (1984) for M31 clusters too, adopting however Brodie and Huchra's [Fe/H]. Direct comparison with these data is displayed in Fig. 9 assuming for the models an age of 15 Gyr. In order to

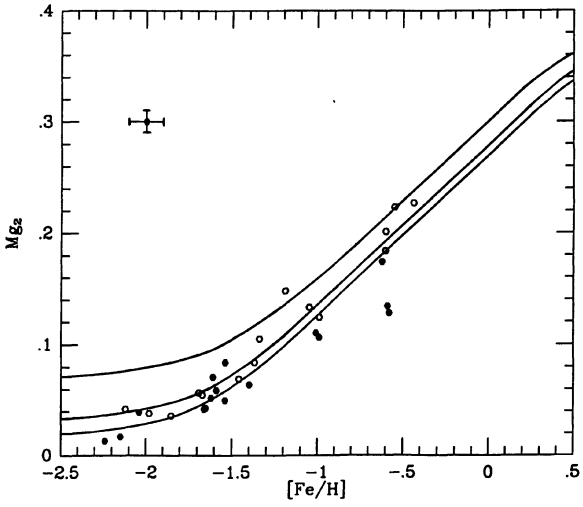

FIG. 9. Calibration of Mg_2 vs [Fe/H] for SSP models. Solid lines display the locus expected for 15 Gyr populations with IMF exponent equal to 1.35 (lower line) 2.35 (central line), and 3.35 (upper line). Full and open dots represent Galactic and M31 globular clusters, respectively. Data are from Burstein *et al.* (1984) while metallicity scale is from Brodie & Huchra (1990). Typical error bars are displayed top left.

slightly refine the match with the clusters we maintained a red HB morphology only for metal-rich models (i.e. $[Fe/H] \geqslant -1$) adopting otherwise an intermediate HB (I-HB) in the notation described in Buzzoni (1989). As discussed above, such a difference is not relevant for the index but can assure a more realistic fit of the data.

The expected derivative of the index versus [Fe/H] from Eq. (8), $\partial Mg_2/\partial [Fe/H] = 0.135$, is only slightly steeper than the empirical value fitted by Brodie & Huchra (1990) who found $\partial Mg_2/\partial [Fe/H] = 0.10$ considering both Galactic and M31 globular clusters. This result is to be considered consistent since in Eq. (8) we restricted only to $[Fe/H] \geqslant -1$ avoiding the *plateau* evident in Fig. 9, as the index approaches the extreme metal-poor regime.

Much larger discrepancies occur, on the contrary, comparing with the calibration proposed by Terlevich *et al.* (1981). If one plots their Eq. (1) on our Fig. 9 it seems that the slope $\partial Mg_2/\partial [Fe/H] = 0.26$ is clearly steeper even respect to the trend inferred from metal-rich globulars alone, and a large offset on the zero point would be required to account for the observations.

Although the precise source of such an apparent inconsistency is hard to be investigated, nevertheless we are inclined to believe that this is a combined effect of both a change in the metallicity scale adopted for the primary calibrators and a rather involved operation translating from different indices. Authors in fact come to their Eq. (1) starting from the Spinrad & Taylor (1969) and Mould (1978) index D(5175) transformed into Mg_2 through an intermediate step via the index Mg_0 used by Burstein (1979). As correctly pointed out by Burstein (1979), that calibration had to be taken as tentative for $[Fe/H] > -0.5$.

The more direct evidence of our comparison with the globular clusters is that Mg_2 seems to consistently trace the global metal content. This means among others that (i) [Mg/*M*] (being *M* the global metallicity) in Galactic and M31 globulars should be not significantly different from the Galactic disk population (as our calibration rests indeed on those stars), and (ii) that [Mg/*M*] is close to zero as the standard theoretical isochrones are able to correctly fit the data.

Our conclusions do not fully support therefore the possibility for a non-solar chemical partition suggested for some extragalactic objects (Burstein *et al.* 1984; Burstein 1985; Efstathiou & Gorgas 1985; Matteucci & Brocato 1990). On the other hand, as investigated in detail by Chieffi *et al.* (1991), the effects of a selective change in the α-elements could work in different ways depending whether or not the variations in the CNO and [Mg + Si + Fe] elements are coupled. On the basis of the available calculations we would not expect any relevant bias in our Mg_2 inferred metallicity scale if only the CNO elements are enhanced. In that case, only stars in the upper main sequence would be affected, and not the cool stars contributing to the Mg blend.

On the contrary, if also Mg is enhanced this would increase the bound-free opacity in the atmosphere of the red giants inducing therefore a stronger Mg_2 index (as well as redder colors). As a consequence, only in that case we would overestimate the true metallicity.

In Fig. 10 we calculated the Mg_2 distribution from the exhaustive sample of local ellipticals observed by Davies *et al.* (1987). The 460 galaxies with measured Mg_2 display a skewed distribution with mode 0.31, mean 0.29, and standard deviation $\sigma(Mg_2) = \pm 0.03$. The largest value in the sample is 0.384 for NGC 1270 while only three galaxies have exceedingly low values. They are NGC 3156 ($Mg_2 = 0.105$), NGC 404 (0.092), and NGC 5102 (0.005). All of them are recognized to be active galaxies with signs of ongoing star formation. Some other known active galaxies can be recognized among those in the left wing of the distribution for $Mg_2 \leqslant 0.20$, so that we can set at this level a prudent lower break selecting *bona fide* quiescent normal ellipticals. Since the typical uncertainty in the Davies *et al.* (1987) measurements is about ± 0.01, i.e., well below the quoted spread of the data distribution, we have to conclude that elliptical galaxies do display a spread in metallicity.

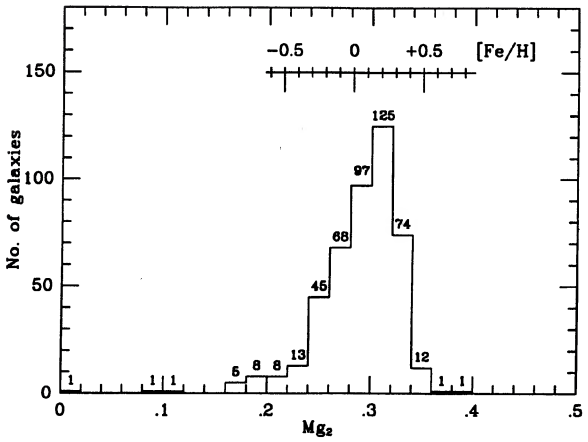

FIG. 10. Metallicity calibration for elliptical galaxies in the Davies *et al.* (1987) sample. Galaxies are assumed 15 Gyr old with a canonical Salpeter IMF.

Our adopted final calibration is reported in the figure. Normal galaxies are assumed to be represented by 15 Gyr SSPs with a canonical Salpeter IMF. We derive that representative values for [Fe/H] are +0.21 at the mode of the distribution or +0.06 at the mean, with a spread of ± 0.22 dex. Note that decreasing the assumed age by a factor of 2 will increase inferred [Fe/H] by 0.36 dex while a variation $\Delta s = \pm 1$ acts conversely on [Fe/H] with a change about 0.12 dex. Normal ellipticals seem therefore to have a mean metallicity enhanced by 20%–60% respect to the solar value spanning over one order of magnitude at the extreme edges of their assumed fiducial distribution.

We can summarize our results combining in a general view both galaxies and globular clusters. Figure 11 collects all those objects from the previous sources for which we have confident IR colors. Dereddened $V-K$ data for ellipticals were taken from Frogel *et al.* (1978), while colors for Galactic and M31 clusters were recompiled by Burstein *et al.* (1984) resting on the original observations by Aaronson & Malkan (1983) and Frogel *et al.* (1980).

When dealing with infrared colors one should consider carefully the effects of stellar mass loss in the SSP models. Stars at the tip of RGB and AGB could strongly change their contribution to the integrated $V-K$ of a SSP depending on the mass loss rate assumed [on the contrary, Mg_2 is not affected so sensitively as it can be seen in Tables 3(a)–3(c)]. Since from Galactic globular clusters we have direct evidence that mass loss works in such a way to equalize the luminosity of the stars at the tip of RGB and AGB (Fusi

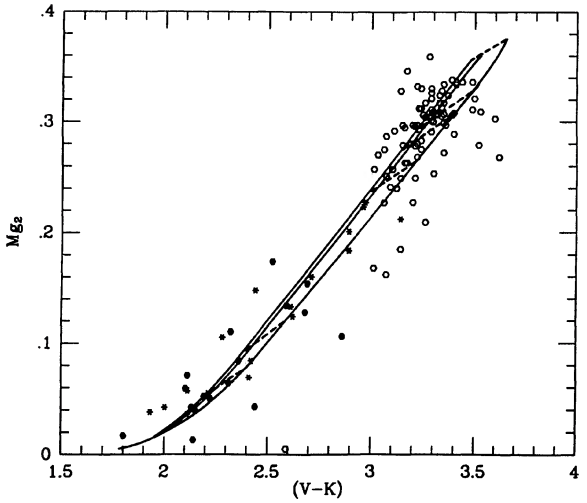

FIG. 11. Adopted calibration for Mg_2 in stellar systems. Upper, central, and lower lines are, respectively, for 15 Gyr SSPs with $s = 1.35$, 2.35, and 3.35. Dashed lines within the strip mark increasing metallicity $Z = 0.0001$, 0.001, 0.01, 0.017, 0.03, and 0.1. Open dots are elliptical galaxies from Davies *et al.* (1987), while full dots and asterisks are Galactic and M31 globular clusters are from Burstein *et al.* (1984). See text for details and discussion.

Pecci & Renzini 1978) we extended this constraint also to galaxies attempting a fit over such a wide set of different stellar systems. Our final adopted calibration for Mg_2 in stellar systems is given in Table 4, together with the corresponding broadband colors, and for different IMFs. A compact formula that fits the case of a Salpeter IMF and could be useful in the range of the elliptical galaxies is

$$Mg_2 = 0.135[\mathrm{Fe/H}] + 0.28. \quad (9)$$

6. THE AGE–METALLICITY DILEMMA

Considering in further detail our previous calibration involving old SSPs it could be questioned that our assumption about galactic age could be arbitrary, and possibly even wrong on the basis of claimed evidences for extensive activity of star formation in elliptical galaxies at more recent epochs (O'Connell 1980; Pickles 1985). In case, spectrophotometric properties of galaxies should be dominated by young SSPs with age typically about 5 Gyr. Such a controversy is part of what we refer to as the "age–metallicity dilemma." The ambiguity is due to the fact that integrated photometric features marking age of the stellar populations are often also metal dependent so that one cannot firmly overcome a potentially misleading interpretation of the data.

As we discussed previously, recent (or even ongoing) stellar activity in ellipticals, does not seem to be a so common event, and in case galaxies do clearly display a peculiar behaviour in the UV part of their SED (Burstein *et al.* 1988a).

The Mg_2 index, coupled with a broadband color, like $V - K$ for example, can help disentangling the problem, due to its different combined response to age and metallicity. This is sketched in Fig. 12, where the different behaviour of Mg_2 versus age and [Fe/H] is displayed. One clearly sees that 5 Gyr stellar populations cannot fairly account for observed properties unless to suppose very *ad hoc* conditions. Actually, only the bluest "active" galaxies, as we mentioned in previous section, can be matched with some confidence.

A possible relevant exception evident in the figure is the case of M32. The dwarf companion of the Andromeda galaxy is clearly displaced to lower values both of Mg_2 and $V - K$ with respect to the bulk of the galaxy distribution. On the basis of Table 4 one would suggest for this galaxy an exceedingly low value for [Fe/H] possibly about -0.5 in marginal disagreement with other studies resting on population synthesis and supporting more enhanced values about or slightly less than the solar metallicity (Faber & French 1980; Boulade *et al.* 1988). It is such a peculiar "blueness" indeed that led people to claim for this galaxy an extensive star formation at recent epochs indirectly supporting in a more general view a young-population scenario for elliptical galaxies (O'Connell 1980).

Due to the importance of the question it is worth spending here some more words in regard. Although in the $Mg_2/(V - K)$ plane M32 is marginally located in the "forbidden" zone populated by the star-forming galaxies, as we discussed in the previous section, nevertheless we take the

TABLE 4. Adopted calibration vs [Fe/H].

	s=1.35			s=2.35			s=3.35		
[Fe/H]	Mg_2	$B-V$	$V-K$	Mg_2	$B-V$	$V-K$	Mg_2	$B-V$	$V-K$
−2.50	0.020	0.58	2.04	0.033	0.61	2.12	0.072	0.65	2.35
−2.00	0.030	0.60	2.12	0.042	0.62	2.20	0.080	0.66	2.40
−1.50	0.061	0.65	2.29	0.073	0.67	2.35	0.104	0.70	2.54
−1.00	0.124	0.73	2.51	0.137	0.75	2.57	0.160	0.78	2.77
−0.50	0.197	0.82	2.81	0.208	0.84	2.87	0.228	0.87	3.06
0.00	0.270	0.91	3.16	0.280	0.93	3.20	0.300	0.96	3.40
0.25	0.304	0.96	3.32	0.315	0.97	3.37	0.336	1.01	3.55
0.50	0.336	1.00	3.41	0.344	1.01	3.45	0.360	1.04	3.61

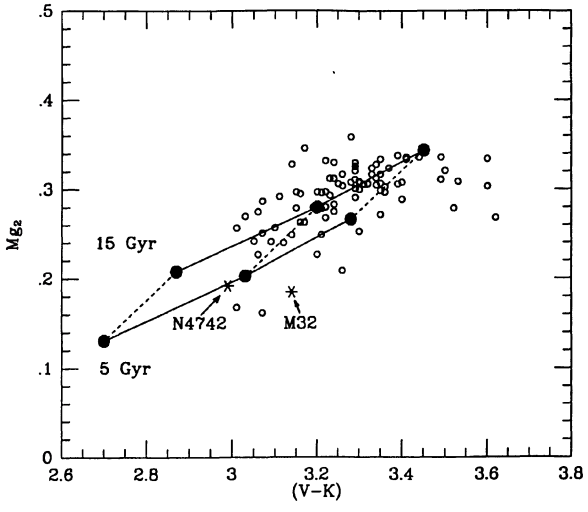

FIG. 12. Comparison between observed galaxies (Davies *et al.* 1987) and expected locus for 15 Gyr (upper solid line) and 5 Gyr (lower line) SSPs with canonical Salpeter IMF. Full dots mark increasing metallicity [Fe/H] = −0.5, 0.0, and +0.5 from the left to the right. See text for discussion about M32 and NGC 4742.

view that the reasons of such a peculiar location are quite different. An illuminating comparison in this regard can be performed with NGC 4742 (marked as well in Fig. 12). The UV properties of this star-forming galaxy have been discussed in detail by Burstein *et al.* (1988a). Its observed UV color is $(1500 - V) = 3.06$ while $Mg_2 = 0.192$. From Persson *et al.* (1979) we have also $(V - K) = 2.99$. For M32 Burstein *et al.* (1988a) give $(1500 - V) = 4.50$, while $Mg_2 = 0.185$ from Davies *et al.* (1987) and $(V - K) = 3.14$ from Frogel *et al.* (1978).

As it can be seen, NGC 4742 fall close to M32 in the diagram of Fig. 12 but *as far as the UV SED is concerned (see Fig. 1 in Burstein et al. 1988a) there is a fundamentally different trend.* In the UV/Mg_2 plane in facts M32 smoothly continues the sequence of quiescent elliptical galaxies whereas NGC 4742 clearly displays its peculiarity lying well off the sequence. This different behavior is witnessing in our opinion that the bulk of the stellar population in M32 is *not* contaminated by young stars but rather than by an old metal-poor stellar component. Actually, this is well evident also in the C–M diagram recently obtained by Freeman (1989) where the scatter in the resolved RGB seems to be induced by a spread in [Fe/H] (see her Fig. 9) with stars as poor as [Fe/H] ~ -1.7.

Just as an instructive exercise with the help of Table 4, one could see that the colors and the Mg_2 index of M32 can be fairly well reproduced by simply adding to a solar population a 30%–40% contribution (in V light) from a 15 Gyr SSP with [Fe/H] $= -1.5$.

7. REDDENING

A by-product of our analysis resting on the combined study of Mg_2 and broadband colors is the possibility to measure the internal reddening of the galaxies. Since the Mg_2 index is virtually a reddening-free feature, in Figs. 11–12 galaxies can only be spread out by Galactic and/or internal reddening along horizontal vectors increasing the broadband colors. A similar approach was first used by Burstein & Heiles (1982, see their Fig. 1) in their work on the Galactic absorption, coupling the Mg_0 index with a color equivalent to $B - R$.

To investigate this matter, we considered the 38 galaxies for which Frogel *et al.* (1978) and Persson *et al.* (1979) supplied multicolor photometry while Mg_2 was measured by Davies *et al.* (1987). The original set of data was corrected for Galactic reddening homogeneously by the different authors using the absorption-free polar-cap model for A_V given by Sandage (1973).

Using our adopted calibration, the following relations can be derived for the color indices of the galaxies ($s = 2.35$):

$$(B - V)_0 = 1.23Mg_2 + 0.58, \quad (10)$$

$$(V - K)_0 = 4.17Mg_2 + 2.025. \quad (11)$$

Color residuals for the relevant galaxies in the sample can be calculated as $\Delta(B - V) = (B - V)_{obs} - (B - V)_0$ and $\Delta(V - K) = (V - K)_{obs} - (V - K)_0$ entering the equations with the observed Mg_2 for each object. The $\Delta(B - V)$ vs $\Delta(V - K)$ is plotted in Fig. 13. Three remarks can be drawn: (i) there is a clear positive correlation between residuals; (ii) the correlation is such as $\Delta(V - K) = 3\Delta(B - V)$ in perfect agreement with the canonical Galactic reddening law; and (iii) the data clump around zero. It is worth noting that points (i) and (ii) rest uniquely on the correctness of the slope assumed for the Mg_2–color relation, while point (iii) depends also from the zero point of the calibration. We stress that our slopes are theoretical expectations and *not* a fit to the data. Fully equivalent conclusions could be achieved however using the empirical relation suggested by Burstein *et al.* (1988b).

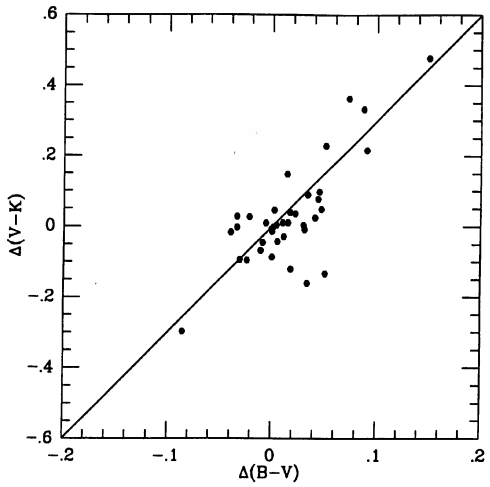

FIG. 13. Color residuals galaxies in the Frogel *et al.* (1978) and Persson *et al.* (1979) sample respect to Eqs. (10) and (11) (38 galaxies). A clear correlation is evident with the solid line displaying the trend expected for Galactic reddening.

Focusing our attention only on $V - K$ we can compute the color residuals with respect to Eq. (11) for 80 galaxies from the previous sources displayed in the histogram of Fig. 14. From the figure, one derives a standard deviation $\sigma(V - K) = \pm 0.13$ mag, fully comparable with the photometric uncertainties in the measurements originally quoted by authors. This, together with the fact that residuals peak around zero, seems to suggest that the intrinsic color excess of the galaxies is probably low, typically less than $E(B - V) \sim 0.04$, and possibly equal zero. Such a conclusion supports the work by Bruzual *et al.* (1988) based on the theoretical solution of the equation for radiative transfer simulating dusty galaxies.

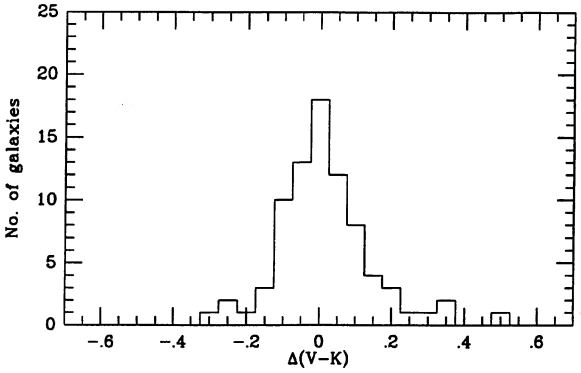

FIG. 14. Same as Fig. 13 but plotted as histogram of the $V - K$ residuals (80 galaxies available). The scatter of the distribution is $\sigma = \pm 0.13$ mag. See text for discussion.

8. OPENING TO COSMOLOGY

A number of investigations are converging toward a unitary view of the evolutionary properties of the elliptical galaxies (Terlevich *et al.* 1981; Edmunds & Phillips 1989). Such a combined approach tracking objects in a multidimensional phase space rests basically on a measure of luminosity (absolute magnitudes), mass (surface brightness or density), and metallicity (colors or spectral indices), and embodies in principle well recognized partial correlations like for instance the color–luminosity (Sandage & Visvanathan 1978), the luminosity-surface-brightness/velocity dispersion (Kormendy 1977; Faber & Jackson 1976), and the density–metallicity relations (Edmunds & Phillips 1989).

In this respect the Mg_2 index can be a very effective tool since it closely relates both to luminosity and mass of galaxies via a complementary measure of their velocity dispersion (Terlevich *et al.* 1981) or surface brightness (De Carvalho & Djorgovski 1989). Actually, such a fair correlation led De Carvalho & Djorgovski (1989) to use Mg_2 for a new family of distance indicators alternative and as reliable as the Tully–Fisher (1977, TF) relation. In their work Mg_2 enters both for an absolute measure of the size and magnitude of galaxies. Like the TF relation however, this can be applied only locally to derive the distance moduli for bright galaxies allowing an estimate of the Hubble constant (H_0).

Looking further into the possibility of using the Mg_2 index as a cosmological tool we might imagine a test involving the observation of the index in the distant galaxies. As we could follow its evolution in the elliptical galaxies in principle we could link the look-back time with redshift, therefore tracing the space time.

We are aware of course that also this test is not free from potential biases. The definition of Mg_2 for distant galaxies is at present a difficult task, due not only to the unfavorable faintness of the objects but mainly to the lack of proper templates at those magnitude levels. This could be a serious problem since the index was originally defined on bright unfluxed templates at $z = 0$, and any attempt to overlap with high-redshift objects should account also for the different detector response by changing the apparent wavelength of the Magnesium feature. Moreover, a further warning deals of course with any possible computational and/or philosophical uncertainties that might affect our inferences based on models for population synthesis.

In Fig. 15 we display the expected variation of Mg_2 with redshift for different cosmological models. The three panels account for some relevant sets of parameters; panels (a) and (b) explore the two extreme cases of an empty ($\Omega_0 = 0$) and an Einstein–De Sitter ($\Omega_0 = 1$) Universe with zero-cosmological constant (Λ_0). The third panel accounts for the inflationary case in a zero-curvature metrics [i.e., $\Omega_0 + \lambda_0 = 1$, where $\lambda_0 = 2/3\Lambda_0(c/H_0)^2$] assuming $\Omega_0 = 0.1$. In all cases two families of curves are displayed according to values of 50 and 100 km/s/Mpc for the Hubble constant, and three choices for the redshift of galaxy formation ($z_f = \infty, 5, 3$).

It could be argued that the feasibility of the test is seriously affected by the intrinsic spread in metallicity among the single galaxies. In fact, as one can see from Eq. (8) and Fig. 10 adopting the spread $\sigma(Mg_2) = \pm 0.03$ observed for present-day galaxies, time resolution is blurred by more than 53%. However, a better accuracy would be obtained using homogeneous groups of galaxies at the same distance as it is

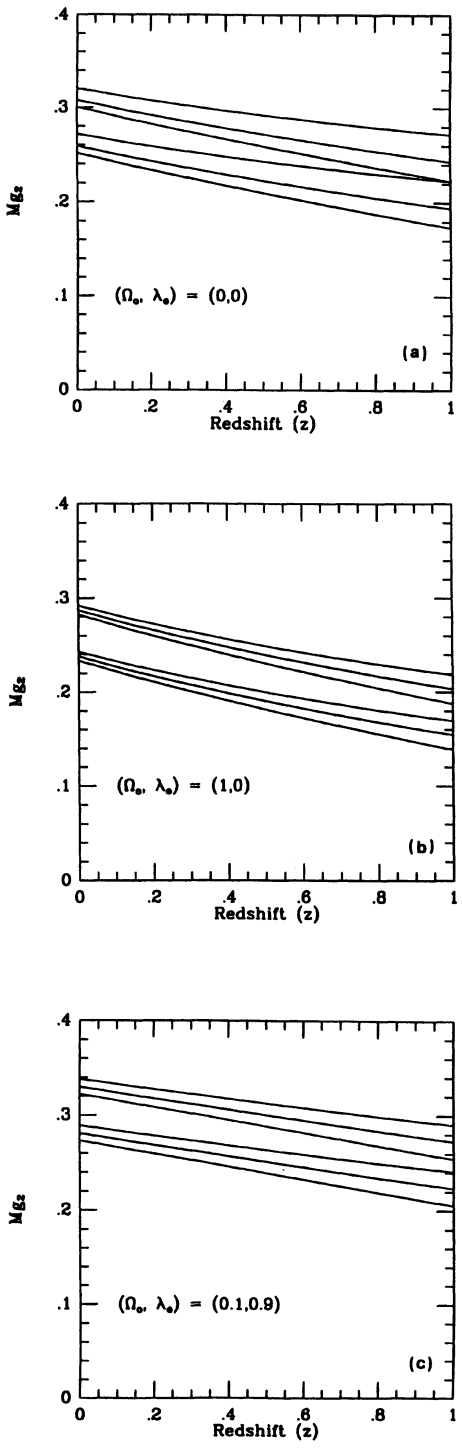

FIG. 15. (a)–(c) Expected variation of the Mg_2 index in distant galaxies according to three different models of the Universe. In each panel calculations are shown for two values of the Hubble constant equal to 50 (upper sheaf of lines) and 100 km/s/Mpc (lower lines), and three values for the redshift of galaxy formation $z_f = 3$, 5, and ∞ (from the lower to the upper line in each sheaf, respectively). Assumed cosmological parameters are reported in each panel and are discussed in the text. Models in (c) could account for inflationary scenarios in a zero-curvature space.

the case for the clusters. For example, averaging over a sample of 10 objects we could derive $\langle Mg_2 \rangle$ within 1% reaching a resolution as good as 15% on the inferred look-back time.

It is worth remarking that this is a basically different approach to observational cosmology respect to the TF test because we implicitly search for a measure of the cosmological *clock* while TF focuses on a measure of the local *distance* scale. This is why both H_0, Ω_0, and Λ_0 are involved at a time in our case.

9. CONCLUSIONS

In this work we approached the problem of a quantitative calibration of the Mg_2 index. At present, such a project still imposes as a crucial step toward a confident estimate of the effective metallicity of the stellar populations in elliptical galaxies. There are many advantages in working with this index. Observations are facilitated since the absorption feature falls in the visual wavelength range, and emerges very sharply in the spectra of the galaxies; moreover, Mg_2 carries integrated information from cool stars (both giants and dwarfs) in the stellar populations, and its theoretical study can be pursued in principle by means of canonical procedures for spectral population synthesis.

Two main difficulties still remain to be properly settled. From the observational point of view we lack a reliable grid of faint stellar/galactic templates allowing to extend the measure of the index up to very distant objects such as high-redshift galaxies. Moreover, in these cases the link to standards cannot be performed directly on the basis of unfluxed spectra but it requires to calibrate both targets and standards in a consistent way to account for redshift and consequent differences in the detector response.

Concerning the theoretical side, Mg_2 is still hardly synthesized via stellar model atmospheres. The reason rests on the fact that it comes from a blend of atomic and molecular contributions, and we know how difficult it is to handle molecules in the models, especially attempting the synthesis of cool stars (Gulati *et al.* 1991). In this case a twofold difficulty arises since molecular contribution appears both in the Magnesium feature and in the side pseudo-continuum mainly due to TiO and CN (Barbuy 1989).

In this work we used a combined approach of theory and observation. To derive a reliable calibration for stellar populations as a whole we first got a calibration versus the fundamental distinctive parameters of single stars. This has been done empirically looking at real stars for which reasonably good estimates are available for temperature, gravity and metallicity. Our final calibration suitable for stars is summarized in Eqs. (4) and (5), where we also give the direct dependence of the index on metallicity on the basis of the empirical stellar database.

The subsequent step toward galaxies required to obtain the synthetic index for stellar populations exploring the complex phase space of their distinctive parameters. This has been accomplished for a wide combination of ages, IMFs, and metallicities by means of theoretical models for SSPs resting on Buzzoni's (1989) computational code. Focusing on observed properties of the galaxies and globular clusters, we converged into an absolute calibration given in Eqs. (8) and (9).

Elliptical galaxies are fairly well reproduced, still supporting the evidence for old metal-rich stellar systems. Their age seems to be consistent with 15 Gyr, and metallicity should exceed the solar value, with [Fe/H] typically about $+0.15$ but with a large spread, nearly one order of magnitude, among single galaxies. This confirms that it is metallicity (and not age, for instance) the driving parameter determining the color distribution of the galaxies. Combining the analysis of the Mg_2 index with the apparent $B-V$ and $V-K$ colors of the galaxies in a way similar to that of Burstein & Heiles (1982) we were able to conclude that the color excess across elliptical galaxies is low, and consistent with zero, as inferred also by Bruzual *et al.* (1988) on the basis of a theoretical argumentation.

Finally, the possible use of Mg_2 for cosmological aims has been quickly analyzed, and here we give some predictions about the expected trend of the index in distant galaxies according to three relevant models of Universe, one of which accounting for a plausible inflationary scenario. The expected variations of the index versus redshift are not so large, but a test in this sense could be successfully accomplished in our opinion looking at clusters of galaxies. Present technological capabilities are probably able to reach the desired accuracy, once the *caveat* about faint templates, as mentioned above, could be fulfilled.

Enjoyable interactions with many colleagues contributed some of the ideas in this work. Fruitful discussions with M. Lucia Malagnini and Ravi Gulati, in Trieste, helped in refining our strategy in this project, allowing to clarify some preliminary questions on the theoretical side dealing with the model atmospheres. Francesca Matteucci and John Danziger at ESO are also acknowledged for having timely pointed out some relevant questions dealing with the galactic chemical mix. Finally, thanks are due to the anonymous referee who contributed with stimulating suggestions to the improvement of this work.

REFERENCES

Aaronson, M., & Malkan, M. 1983, private communication by Burstein *et al.* (1984) (see below)
Aaronson, M., Cohen, J. G., Mould, J., & Malkan, M. 1978, ApJ, 223, 824
Barbuy, B. 1989, Ap&SS, 157, 111
Becker, S. A. 1981, ApJS, 45, 475
Boulade, O., Rose, J. A., & Vigroux, L. 1988, AJ, 96, 1319
Brodie, J. P., & Huchra, J. P. 1990, ApJ, 362, 503
Bruzual, G., Magris, G., & Calvet, N. 1988, ApJ, 333, 673
Burstein, D. 1979, ApJ, 232, 74
Burstein, D. 1985, PASP, 97, 89
Burstein, D., & Heiles, C. 1982, AJ, 87, 1165
Burstein, D., Faber, S. M., Gaskell, C. M., & Krumm, N. 1984, ApJ, 287, 586
Burstein, D., Bertola, F., Buson, L., Faber, S. M., & Lauer, T. R. 1988a, ApJ, 328, 440
Burstein, D., Davies, R. L., Dressler, A., Faber, S. M., Lynden-Bell, D., Terlevich, R., & Wegner, G. 1988b, in Towards Understanding Galaxies at Large Redshift, edited by R. Kron & A. Renzini (Kluwer, Dordrecht), p. 17
Buzzoni, A. 1988, in Towards Understanding Galaxies at Large Redshift, edited by R. Kron & A. Renzini (Kluwer, Dordrecht), p. 61
Buzzoni, A. 1989, ApJS, 71, 817

Cayrel de Strobel, G., Bentolila, C., Hauck, B., & Duquennoy, A. 1985, A&AS, 59, 145
Chieffi, A., Straniero, O., & Salaris, M. 1991 in The Formation of Star Clusters, ASP Conference Series, edited by K. Janes (ASP, San Francisco), Vol. 13, p. 219
Davies, R. L., Burstein, D., Dressler, A., Faber, S. M., Lynden-Bell, D., Terlevich, R. J., & Wegner, G. 1987, ApJS, 64, 581
De Carvalho, R. R., & Djorgovski, S. 1989, ApJ, 341, L37
Edmunds, M. G., & Phillips, S. 1989, MNRAS, 241, 9p
Efstathiou, G., & Gorgas, J. 1985, MNRAS, 215, 37p
Faber, S. M., & Jackson R. 1976, ApJ, 204, 668
Faber, S. M., & French, H. B. 1980, ApJ, 235, 405
Faber, S. M., Burstein, D., & Dressler, A. 1977, AJ, 82, 941
Faber, S. M., Friel, E. D., Burstein, D., & Gaskell, C. M. 1985, ApJS, 57, 711
Freeman, W. L. 1989, AJ, 98, 1285
Frogel, J. A., Persson, S. E., & Cohen, J. G. 1980, ApJ, 240, 785
Frogel, J. A., Persson, S. E., Aaronson, M., & Matthews, K. 1978, ApJ, 220, 75
Fusi Pecci, F., & Renzini, A. 1978, in The HR Diagram, IAU Symposium No. 80, edited by A. G. D. Philip & D. S. Hayes (Reidel, Dordrecht), p. 225
Gulati, R. K., Malagnini, M. L., & Morossi, C. 1991, A&A, 247, 447
Kormendy, J. 1977, ApJ, 218, 333
Matteucci, F., & Brocato, E. 1990, ApJ, 365, 539
Mould, J. R. 1978, ApJ, 220, 434
O'Connell, R. W. 1980, ApJ, 236, 430
Persson, S. E., Frogel, J. A., & Aaronson, M. 1979, ApJS, 39, 61
Pickles, A. J. 1985, ApJ, 296, 340
Reimers, D. 1975, Mem. Soc. Roy. Sci. Liège, 6th Ser., 8, 369
Rose, J. A. 1985, AJ, 90, 1927
Sandage, A. R. 1973, ApJ, 183, 711
Sandage, A. R., & Visvanathan, N. 1978, ApJ, 225, 742
Spinrad, H., & Taylor, B. J. 1969, ApJ, 157, 1279
Terlevich, R., Davies, R. L., Faber, S. M., & Burstein, D. 1981, MNRAS, 196, 381
Tully, B., & Fisher, J. 1977, A&A, 54, 661
VandenBerg, D. A. 1985, ApJS, 58, 711
Veeder, G. J. 1975, AJ, 79, 1056
Zinn, R., & West, M. 1984, ApJS, 55, 45